

**A STUDY OF MARINE STRATOCUMULUS USING LIDAR  
AND OTHER FIRE AIRCRAFT OBSERVATIONS**

Jørgen B. Jensen and Donald H. Lenschow

National Center for Atmospheric Research <sup>1</sup>

Boulder, Colorado 80307

**1. BACKGROUND**

In order to understand the distribution and evolution of marine stratocumulus, we need to determine how variables such as radiation divergence, surface heat and moisture fluxes, wind shear, subsidence, and lapse rate control the dynamical and microphysical structure of the clouds through processes such as entrainment and mixing, and in turn, how the cloud structure affects these variables. A key to studying entrainment is to be able to resolve the structure of the cloud at and near cloud-top. Ideally, we would like to be able to resolve both the motion field as well as some tracer that allows us to distinguish well-mixed boundary-layer air from that originating in the free atmosphere and entrained into the boundary layer. At the top of the stratiform-capped boundary layer, the cloud itself can be a tracer of boundary-layer air. Entrained parcels, or regions of mixed boundary-layer and free air are clear. The NCAR Airborne Infrared Lidar (NAILS, Schwiesow, 1987) is a tool for distinguishing the interface between the clear and cloudy parcels.

Some progress has already been made in studying the characteristics of the entrainment region of marine stratocumulus. Jensen and Lenschow (1978), for example, investigated the sizes of turbulent eddies at the top of a cloud-capped mixed layer using data from an aircraft flight leg at cloud-top. They found two peaks in the vertical velocity spectrum at cloud-top—one with a wavelength of about 1.5 times the depth of the mixed layer, and the other with a wavelength of 200 to 300 m that likely was associated with entrainment and mixing near cloud-top. Mahrt and Paumier (1982) looked in more detail at the entrainment process at cloud top for the same experiment, and estimated a scale of 100 to 200 m for the eddies involved in cloud-top entrainment. These results have been confirmed in subsequent observational studies by Caughey and Kitchen (1984) for nocturnal stratocumulus over land using tethered balloon observations.

A theoretical analysis of the preferred wavelengths and frequencies of vertical velocity fluctuations in the inversion layer capping a clear-air mixed layer and the interactions of waves and turbulence at the top of the mixed layer has been carried out by Carruthers and Hunt (1985 and 1986), and related numerical simulations are reported by Carruthers and Moeng (1987). Again, these analyses suggest vertical velocity wavelengths of a few hundred meters in the vicinity of the mixed-layer top. From the standpoint that clouds offer a visible tracer of the interface between the free atmosphere and the boundary layer, the cloud-capped boundary layer has an advantage over a clear boundary layer. [We note, however, that occasionally a thin cloud-free layer has been observed just below the capping

---

<sup>1</sup> The National Center for Atmospheric Research is funded by the National Science Foundation.

inversion (e.g. Rogers and Telford, 1986). This situation, although possibly not common, warrants further study to see if differences in cloud-top structure are also detectable with NAILS; we recall, on the basis of our inflight observations, that one or more cases of this situation exist in the FIRE data set.]

Thus far, most of the observational evidence for studies of the eddy size and structure in the vicinity of cloud top has come from direct measurements of vertical velocity, temperature and cloud droplet size distributions. Recently, however, Boers and Spinhirne (1987) have reported lidar observations of cloud top which illustrate some of the potential that this technique has to offer. They show, for example, a frequency distribution and spectrum of cloud-top height for a marine stratocumulus case, and indicate that in situ measurements in cloud were obtained concurrently on a second airplane; the in situ observations are discussed in Boers and Betts (1988).

In addition to investigations in the vicinity of cloud top, the NAILS was also pointed up at cloud base while flying below the stratocumulus. In this way, it is possible to look at cloud-base structure to see how it correlates with measurements in the lower boundary layer. A couple of interesting and important questions that can be addressed are: is the scale of cloud organization seen in cloud-base height detectable in variables measured at aircraft height? How well can the lidar detect multiple cloud layers which, as discussed by Nicholls (1984) and Hanson et al. (1988), are indicative of decoupling of the main cloud layer from the boundary layer, and if detected, can they also be related to variables measured at aircraft height? As Nicholls (1984) points out, this decoupling can make a significant difference in the subsequent evolution of the cloud cover, and therefore significantly affect the radiation budget of the cloud-capped mixed layer.

## 2. NAILS

The NCAR airborne infrared lidar system (NAILS) used in the 1987 FIRE experiment off the coast of California is a  $10.6 \mu\text{m}$  wavelength  $\text{CO}_2$  lidar system constructed by Ron Schwiesow and co-workers at NCAR/RAF. The lidar is particularly well suited for detailed observations of cloud shape; i.e. height of cloud top (when flying above cloud and looking down) and cloud base (when flying below cloud and looking up) along the flight path. Schwiesow et al. (1988) have presented some examples of NAILS lidar data from FIRE.

A detailed discussion of the lidar design characteristics is given by Schwiesow (1987), and only a brief summary is listed here (Table 1). The lidar height resolution of  $\pm 3$  m allows for the distance between the aircraft and cloud edge to be determined with this accuracy; however, the duration of the emitted pulse is approximately  $3 \mu\text{s}$ , which corresponds to a 500 m pulse length. Therefore, variations in backscatter intensities within the clouds can normally not be resolved. Hence the main parameter obtainable from the lidar is distance to cloud; in some cases we may also be able to determine the cloud depth.

During FIRE the lidar was operational on 7 of the 10 Electra flights, and data were taken when the distance between cloud and aircraft (minimum range) was at least 500 m. The lidar was usually operated at 8 Hz, which at a flight speed of  $100 \text{ m s}^{-1}$  translates into a horizontal resolution of about 12 m.

**TABLE 1**  
**NAILS Lidar Characteristics (modified from Schwiesow, 1987)**

Operating wavelength	10.6 $\mu$ m
Beam width	$16 \times 10^{-5}$ radians
Lidar return sampling rate	100 MHz
Height resolution	$\pm 3$ m
Track resolution (variable*)	$\sim 10$ m
Design backscatter coefficient	$5 \times 10^{-9}$ ( $\text{m}^{-1} \text{sr}^{-1}$ )
Maximum range from aerosols	2 km
Maximum range from cloud	5 km
Minimum range (dead zone)	500 m
Signal channels (polarization)	2

\*Depending upon pulse frequency and flight speed.

The backscatter as function of time (equivalent to distance) for each laser pulse is stored in digital form on magnetic tape. Currently, three independent variables are available to the investigators on the FIRE Electra data tapes: lidar range to cloud, strength of return (relative power) and pulse width of return, which is related to penetration depth.

The values of these variables should currently be interpreted with some caution. In the future we hope (i) to test the detection algorithm in order to insure that the actual cloud edge is detected, (ii) to determine under what circumstances the lidar is able to detect the heights of both cloud base and cloud top, and (iii) to correct the data for pitch and roll errors.

### 3. EXAMPLES OF NAILS DATA

The following example illustrates only one of many ways the lidar can be used in conjunction with other sensors in order to study stratocumulus clouds. Schwiesow *et al.* (1988) present time series of lidar-derived cloud top height and radiation temperature at cloud top from the Barnes PRT-5 sensor. Fig. 1 shows the cloud top height,  $z_c$ , measured by the Electra from 211100 to 211400 PDT on June 30, 1987. The lidar shows numerous variations in the cloud top height on scales of hundreds of meters. In the following we will examine the association between the variation of cloud top height and cloud top temperature.

In Fig. 1 we have selected a segment of the cloud top for calculating a reference value of entropy. If we assume a moist adiabatic temperature gradient in the cloud, then we can calculate the temperature of the cloud surface based on the lidar measured cloud top height. This lidar-derived cloud top temperature,  $T_l$ , can then be compared with the PRT-5 temperature,  $T_r$ ; see Fig 1, center panel. Differences between these two,  $\Delta T = T_r - T_l$ , are shown in the bottom panel of Fig. 1 and they can be due to several effects:

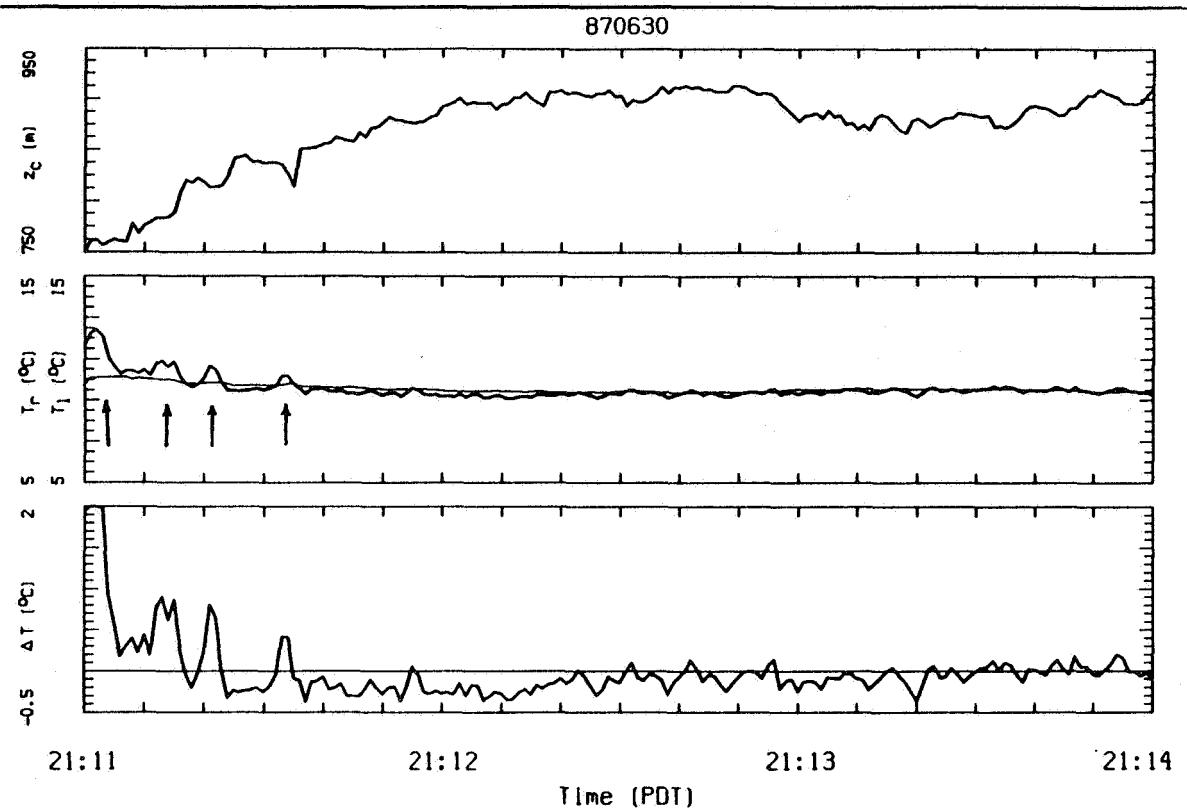


Fig. 1. Top panel: Lidar-derived cloud top height ( $z_c$ ) averaged to  $1 \text{ s}^{-1}$ . Middle panel: PRT-5 radiation temperature ( $T_r$ , bold line) and lidar-derived cloud top temperature ( $T_l$ , thin line). See text for explanation of arrows. Bottom panel: Temperature difference,  $\Delta T = T_r - T_l$ . The thin line shows  $\Delta T = 0$ . The distance between tick marks on the abscissa is  $\approx 1 \text{ km}$ .

- (1) Radiative cooling and the subsequent formation of cold pools may lead to a pattern in which local depressions in the cloud top surface have predominantly negative  $\Delta T$ .
- (2) Entrainment and the ensuing evaporative cooling may likewise lead to local depressions in the cloud top surface with negative  $\Delta T$ .
- (3) It is not clear to what extent the lidar-derived cloud edge coincides with the region which dominated the PRT-5 signal. If the cloud is very thin, then the PRT-5 temperature may include contributions from a substantial cloud depth, whereas the lidar may detect the actual cloud edge. This would lead to regions of positive  $\Delta T$ .
- (4) The approximation of moist adiabatic temperature gradient may not be valid for the cloud.

An examination of Fig. 1 does not result in obvious correlations between  $z_c$  and  $\Delta T$ ; hence without further investigation we can not conclude that "domes" contain warm air, whereas depressions between them contain cooled air. Examples of "thin" cloud appear likely in at least four segments, as indicated by the arrows in Fig. 1.

## REFERENCES

Boers, R. and A.K. Betts, 1988: Saturation point structure of marine stratocumulus clouds. Preprint Volume, Seventh Conference on Ocean-Atmosphere Interactions of the AMS, 1-5 February 1988, Anaheim, CA. American Meteorological Society, Boston, MA, 166-169.

Boers, R. and J.D. Spinhirne, 1987: High altitude lidar observations of marine stratocumulus clouds. Topical Meeting on Laser and Optical Remote Sensing: Instrumentation and Techniques Technical Digest Series, 1987 Volume 18, (Optical Society of America, Washington, D.C.) 84-87.

Carruthers, D.J. and J.C.R. Hunt, 1985: Turbulence and wave motions near an interface between a turbulent region and a stably stratified layer. *Turbulence and Diffusion in Stable Environments*, edited by J.C.R. Hunt, Clarendon Press, Oxford, 319 pp.

Carruthers, D.J. and J.C.R. Hunt, 1986: Velocity fluctuations near an interface between a turbulent region and a stably stratified layer. *J. Fluid Mech.*, 165, 475-501.

Carruthers, D.J. and C.-H. Moeng, 1987: Waves in the overlying inversion of the convective boundary layer. *J. Atmos. Sci.*, 44, 1801-1808.

Caughey, S.J. and M. Kitchen, 1984: Nocturnal stratocumulus. *Quart. J. Roy. Met. Soc.*, 110, 13-34.

Hanson, H.P., G.K. Greenhut and V.E. Derr, 1988: An investigation of the climatology and mechanics of the California stratocumulus cloud deck. Submitted to *Bull. Amer. Meteor. Soc.*

Jensen, N.O. and D.H. Lenschow, 1978: An observational investigation of penetrative convection. *J. Atmos. Sci.*, 35, 1924-1933.

Lenschow, D.H., I.R. Paluch, A.R. Bandy, R. Pearson, Jr., S.R. Kawa, C.J. Weaver, B.J. Huebert, J.G. Kay, D.C. Thornton and A.R. Driedger III: Dynamics and Chemistry of Marine Stratocumulus (DYCOMS) Experiment. Submitted to *Bull. Amer. Meteor. Soc.*

Mahrt, L and J. Paumier, 1982: Cloud-top entrainment instability observed in AMTEX. *J. Atmos. Sci.*, 39, 622-634.

Nicholls, S., 1984: The dynamics of stratocumulus: Aircraft observations and comparisons with a mixed layer model. *Quart. J. Roy. Meteor. Soc.*, 110, 783-820.

Rogers, D. and J. Telford, 1986: Metastable stratus tops. *Quart. J. Roy. Met. Soc.*, 112, 481-500.

Schwiesow, R.L., 1987: *The NCAR Airborne Infrared Lidar System (NAILS) Design and Operation*, NCAR Technical Note NCAR/TN-291+1A, Available from NCAR, P.O. Box 3000, Boulder CO, 80307, 38 + xiii pp.

Schwiesow, R.L., V.M. Glover and D.H. Lenschow, 1988: Measurements with airborne lidar: an example from FIRE and potential applications to turbulence and diffusion. Preprint Volume, Eighth Symposium on Turbulence and Diffusion of the American Meteorological Society, 26-29 April 1988, San Diego, CA.